Available online at www.sciencedirect.com
SCIENCE DIRECT
Polymer 46 (2005) 6500–6506
polymer
www.elsevier.com/locate/polymer

The structure of poly(ethylene oxide) liquids: comparison of integral equation theory with molecular dynamics simulations and neutron scattering

John G. Curro[a,b,*], Amalie L. Frischknecht[a]

[a]Sandia National Laboratories, P.O. Box 5800, Albuquerque, NM 87185, USA
[b]Department of Chemical and Nuclear Engineering, University of New Mexico, Albuquerque, NM 87131, USA

Received 12 January 2005; accepted 5 March 2005
Available online 24 June 2005

Abstract

Polymer reference interaction site model (PRISM) calculations and molecular dynamics (MD) simulations were carried out on poly(ethylene oxide) liquids using a force field of Smith, Jaffe, and Yoon. The intermolecular pair correlation functions and radius of gyration from theory were in very good agreement with MD simulations when the partial charges were turned off. When the charges were turned on, considerably more structure was seen in the intermolecular correlations obtained from MD simulation. Moreover, the radius of gyration increased by 38% due to electrostatic repulsions along the chain backbone. Because the partial charges greatly affect the structure, significant differences were seen between the PRISM calculations (without charges) and the wide angle neutron scattering measurements of Annis and coworkers for the total structure factor, and the hydrogen/hydrogen intermolecular correlation function. This is in contrast to previous PRISM calculations on poly (dimethyl siloxane).

Keywords: PEO; PRISM theory; MD simulation

1. Introduction

Poly(ethylene oxide) (PEO) is a water soluble polymer that has many important technological applications. It is widely used as a drag reducer [1] in the flow of water in pipes. It has also found applications as a polymer electrolyte [2]. Perhaps the most important applications of PEO are biological since PEO is compatible with human blood and tissue [3]. Because of its importance, PEO has been the subject of numerous theoretical [4–10] and simulation studies [11–17].

In aqueous solution, PEO displays a closed loop phase diagram as a result of hydrogen bonding. PEO in aqueous solution has been modeled with various mean field theories [4–9] to include the effect of hydrogen bonding. Using the associating fluid approach of Semenov and Rubinstein [10], Dormidontova [9] developed a mean field theory that treats both polymer/water and water/water hydrogen bonds. This theory predicts a closed loop phase diagram in good agreement with experiment.

Various force fields have been developed [12,13–18] for PEO based on quantum calculations and the structure of PEO liquids has been studied in several [12,14,15,19–21] molecular dynamics (MD) simulations. Wide angle neutron scattering has been employed in two studies [20,21] to probe the packing of PEO liquids. Smith, Bedrov and coworkers [11] have performed MD simulations of PEO in aqueous solution. Muller-Plathe and van Gunsteren [16] performed simulations of PEO in the presence of lithium ions. Small angle [19] neutron scattering measurements have been carried out to investigate the structure and chain dimensions of PEO/LiI solutions.

In the present investigation we performed polymer reference interaction site model (PRISM) calculations [22] and MD simulations on PEO liquids on an atomistically realistic, explicit atom model using the force field of Smith, Jaffe, and Yoon [18] (SJY). The focus of this work was to

* Corresponding author. Address: Sandia National Laboratories, P.O. Box 5800, Albuquerque, NM 87185, USA. Tel.: +1 505 272 7129.
E-mail address: jgcurro@sandia.gov (J.G. Curro).

0032-3861/$ - see front matter © 2005 Elsevier Ltd. All rights reserved.
doi:10.1016/j.polymer.2005.03.123

test the agreement between theory, simulation, and experiment for the intermolecular pair correlation functions and structure factors. In previous investigations [23,24] theoretical calculations and MD simulations of poly(dimethyl siloxane) (PDMS) liquids were carried out using united atom and explicit atom force fields, with and without partial charges. Surprisingly, it was found that even though the partial charges were of moderate magnitude, they had only a minor effect on the liquid structure and chain dimensions of PDMS. Thus, one might speculate that other oxygen-containing polymers would behave similarly. In this investigation we also examined the effect of partial charges on the structure of PEO liquids. In the next section we briefly describe the application of self-consistent PRISM theory and MD simulation to PEO liquids. In Section 3 we compare theory and simulation in the absence of charge. We then use MD simulation to examine changes in liquid structure and chain dimensions when the partial charges in the SJY force field are turned on. Finally, we compare our theoretical calculations to wide-angle neutron scattering results of Annis and coworkers [20] for both the total structure factor and the intermolecular correlations between H atoms in PEO liquids.

2. Theory and simulation

2.1. PRISM theory

PRISM theory [22,25–28] is an extension to polymers of the reference interaction site model, or RISM theory, of Chandler and Andersen [29,30] for small molecule liquids. The theory has been discussed extensively [22,28] and will only briefly be discussed here as applied to PEO liquids. Within the reference interaction site model, interactions and correlations of macromolecules occur between spherically symmetric interaction sites. For PEO there are three independent, overlapping sites: C, O, and H representing the atoms making up the PEO repeat unit [–CH_2–O–CH_2–]. Basically PRISM theory provides a link between the average intramolecular structure of a single macromolecule and the intermolecular packing in a bulk liquid. The intramolecular structure is characterized by the function

$$\hat{\boldsymbol{\Omega}}_{\alpha\gamma}(k) = \frac{1}{N_\alpha} \sum_{i\in\alpha} \sum_{j\in\gamma} \left\langle \frac{\sin kr_{ij}}{kr_{ij}} \right\rangle \tag{1}$$

where the caret denotes the Fourier transform with wave vector k. For PEO α and γ represent a C, O, or H site, and N_α represents the number of sites of type α on a chain. The brackets denote an average over a single chain, which we carry out using a single chain Monte Carlo simulation. The intermolecular packing of PEO is characterized by the six independent radial distribution functions $g_{\alpha\gamma}(r)$ between sites α and γ on different chains.

The generalized Ornstein-Zernike equation proposed by Chandler and Andersen [22,29,30] relates the intramolecular and intermolecular structure

$$\hat{\mathbf{H}}(k) = \hat{\boldsymbol{\Omega}}(k)\cdot\hat{\mathbf{C}}(k)\cdot[\hat{\boldsymbol{\Omega}}(k) + \hat{\mathbf{H}}(k)] \tag{2}$$

where the total correlation function is defined as

$$H_{\alpha\gamma}(r) = \rho_\alpha\rho_\gamma[g_{\alpha\gamma}(r) - 1] \tag{3}$$

and ρ_α is the density of atoms of type α. The generalized Ornstein-Zernike equation can be viewed as a definition of the six direct correlation functions $C_{\alpha\gamma}(r)$. In this work we approximate these direct correlation functions using the Percus-Yevick closure [22,31]

$$C_{\alpha\gamma}(r) = \{1 - \exp[\beta V^{rep}_{\alpha\gamma}(r)]\}[H_{\alpha\gamma}(r) + 1] \tag{4}$$

which is known to be accurate for polymer liquids with strong repulsions and weak attractions at high density. Previous work [22] demonstrated that PRISM theory and the Percus-Yevick closure works best for repulsive potentials. Hence, in Eq. (4) we employ only the repulsive part of the potential $V^{rep}_{\alpha\gamma}(r)$. This approximation makes use of the well known fact that the structure of a van der Waals liquid is determined primarily by the repulsive component of the pair potential for liquids at high density. However, for liquids with partial charges, the electrostatic interactions may, depending on the magnitude of the charges, influence the pair correlations. We will investigate this question later in this paper.

The SJY force field [18] represents the non-bonded interactions with an exponential-6 and Coulombic potential of the form

$$V_{\alpha\gamma}(r) = V_{\alpha\gamma}(r*), \quad r \le r* \tag{5}$$

$$V_{\alpha\gamma}(r) = \varepsilon\left\{\left(\frac{6}{\zeta-6}\right)\exp[\zeta(1-(r/R_0))] - \left(\frac{\zeta}{\zeta-6}\right)\left(\frac{R_0}{r}\right)^6\right\} + K_c\frac{q_\alpha q_\gamma}{r}, \quad r > r*$$

where $K_c = 332.08$ when the charges are turned on. The exp-6 potential in Eq. (5) is non-monotonic in the repulsive regime and has a maximum at a separation r^*. In the MD simulations, separations of $r < r^*$ are never accessed and this cutoff is not relevant since $V(r^*)/k_BT$ is very large for the PEO model studied here. However, in our PRISM calculations, single chain Monte Carlo simulations using the pivot algorithm [33] are employed and it is important to apply a cutoff r^* at short distances so that no two atoms overlap. The parameters for PEO are given in Tables 1 and 2 based on the SJY [18] force field. In Eq. (4) for the closure we use only the repulsive branch of the exp-6 potential defined analogously to the method of Weeks, Chandler, and Andersen [32] for the Lennard-Jones potential:

$$V^{rep}_{\alpha\gamma}(r) = V^{rep}_{\alpha\gamma}(r*) + \varepsilon, \quad r \le r* \tag{6}$$

$$V^{rep}_{\alpha\gamma}(r) = V^{rep}_{\alpha\gamma}(r) + \varepsilon, \quad r* \le r \le R_0$$

Table 1
Non-bonded exp-6 parameters for PEO from SJY [18]

Atom pair ($\alpha\gamma$)	ε (kcal/mol)	R_0 (d[a]) (Å)	ζ
CC	0.094813	3.8719 (3.10)	11.964
CH	0.051988	3.2741 (2.47)	11.181
HH	0.0098036	3.3698 (2.25)	12.603
CO	0.15257	3.4566 (2.88)	12.364
HO	0.044729	3.2778 (2.53)	12.790
OO	0.20334	3.1991 (2.54)	12.998

[a] The effective hard core diameter d was computed from Eqs (5), (6) and (11).

$$V_{\alpha\gamma}^{\mathrm{rep}}(r) = 0, \quad r \geq R_0$$

In our PRISM calculations the charges are turned off ($K_c = 0$).

Because PEO is a flexible macromolecule, one would anticipate that the intramolecular and intermolecular parts of the problem are coupled, requiring that $\Omega_{\alpha\gamma}(r)$ and $g_{\alpha\gamma}(r)$ be determined in a self-consistent manner [22,33]. To carry out this iterative scheme, we employ a solvation potential $w_{\alpha\gamma}(r)$ acting on a single chain during our Monte Carlo calculation. The purpose of this solvation potential is to mimic the effects of the other chains in the system. Assuming pairwise additivity, $\hat{W}_{\alpha\gamma}(k)$ (in Fourier transform space) can be approximately calculated [22,34,35] from

$$\beta\hat{\mathbf{W}}_{\alpha\gamma}(k) \cong -\sum_{i,j} \hat{\mathbf{C}}_{\alpha i}(k)\hat{\mathbf{S}}_{ij}(k)\hat{\mathbf{C}}_{j\gamma}(k) \tag{7}$$

where the structure factors are defined according to

$$\hat{\mathbf{S}}_{\alpha\gamma}(k) = \rho_\alpha \hat{\mathbf{\Omega}}_{\alpha\gamma}(k) + \hat{\mathbf{H}}_{\alpha\gamma}(k) \tag{8}$$

Thus in our single-chain Monte Carlo simulation, the chain is subject to the pair potential $v_{\alpha\gamma}(r)$ consisting of the bare, excluded volume repulsive potential of Eq. (6), and the attractive solvation potential in Eq. (7) due to the other chains.

$$v_{\alpha\gamma}(r) = V_{\alpha\gamma}^{\mathrm{rep}}(r) + W_{\alpha\gamma}(r) \tag{9}$$

A first approximation is to make use of the Flory ideality assumption [36] which assumes that these two contributions approximately cancel each other out so that a chain in a melt is ideal. A more quantitative treatment, which we follow here, requires us to carry out the full self-consistent computation in the following manner: We first guess the solvation potential and use this in a single-chain Monte Carlo simulation [33] to calculate $\hat{\mathbf{\Omega}}_{\alpha\gamma}(k)$. With $\hat{\mathbf{\Omega}}_{\alpha\gamma}(k)$, we use Eqs. (2) and (4) to solve for $\hat{\mathbf{H}}_{\alpha\gamma}(k)$ and $\hat{\mathbf{C}}_{\alpha\gamma}(k)$. This then allows us to calculate a new solvation potential with Eq. (7), and we continue to iterate until the difference between the new and old solvation potentials becomes very small. It should be mentioned that it is not necessary to perform a new Monte Carlo simulation with each iteration. Reweighting techniques [33] can be used to greatly reduce the number of simulations that need to be carried out during the course of the self-consistent calculation.

Table 2
Partial atomic charges from the SJY [18] force field

Atom (α)	q_α
C	−0.066
H	0.097
O	−0.256

When we carry out the single-chain Monte Carlo simulation, as well as our full MD simulations we use the intramolecular potentials from the SJY force field. The bond stretching and bending potentials are taken to be harmonic

$$V_b = \frac{1}{2}k_b(r - r_0)^2 \tag{10a}$$

$$V_\theta = \frac{1}{2}k_\theta(\theta - \theta_0)^2 \tag{10b}$$

and the parameters were taken from Ref. [18]. Our torsional potentials have the form

$$V_t = \sum_{i=0}^{3} a_i \cos^i(\phi) \tag{10c}$$

and the torsional parameters were extracted from the SJY force field [18] and are listed in Table 3.

2.2. MD Simulations

The simulations were carried out using the LAMMPS parallel MD code [37] on systems containing 100 chains of 105 atoms. Overlapping initial configurations were prepared from randomly placed chains with configurations chosen from the Monte Carlo simulations in our PRISM calculations. The overlaps were then removed by pushing off with a soft non-bonded potential. A time step of 0.4 fs was used with a multiple time step integrator (RESPA) so that forces were calculated every time step for bonded interactions, every two time steps for three and four body interactions, and every four time steps for exp-6 and Coulombic interactions. The long range Coulombic forces were calculated with a particle—particle/particle—mesh Ewald algorithm [38]. The simulations were run at constant density of 0.1010/Å^3 and the temperature was controlled at 318 K with a Nose-Hoover thermostat using a coupling frequency of 0.02 fs^{-1}.

Table 3
Torsional parameters (kcal/mol) in Eq. (10c) extracted from the SJY force field [18]

Torsional angles	a_0	a_1	a_2	a_3
HCOC	0	−1.215	0	1.620
COCO	0.350	0.020	−0.070	0.640
OCCH	0	−0.420	0	0.560
OCCO	1.275	0.025	−2.550	0

3. Results and discussion

Self-consistent PRISM calculations were carried out for PEO liquids at 318 K consisting of chains of 15 monomers (105 atoms) at a density of 0.1010 atoms/Å^3. The partial charges were turned off and only the repulsive branch of the exp-6 potential was used in the PY closure. MD simulations were also performed on this same system using the full exp-6 potential of Eq. (5) ($K_c=0$). Six independent intermolecular radial distribution functions between CC, HH, OO, CO, OH, and CH pairs of sites are needed to completely characterize the packing. Figs. (1) and (2) show a comparison between the PRISM theory and the MD simulation for these radial distribution functions. It can be seen that the agreement between theory and simulation is very good when there are no Coulombic interactions.

We can estimate the effective hard core distance $d_{\alpha\gamma}$ between the various pairs of intermolecular sites from the Barker-Henderson formula [31]

$$d_{\alpha\gamma} = \int_0^\infty \left[1 - \exp\left(-\beta V_{\alpha\gamma}^{\mathrm{rep}}\right)\right] \mathrm{d}r \tag{11}$$

where we use the repulsive exp-6 potential defined in Eqs. (5) and (6). Based on the SJY parameters, the various $d_{\alpha\gamma}$ are shown in Table 1. Examination of Figs. (1) and (2) reveals that all the pair correlations $g_{\alpha\gamma}(r)$ start to become non-zero at distances near $d_{\alpha\gamma}$. This indicates that the backbone sites can come into contact with each other and are not completely screened out by the pendant hydrogen atoms.

Note that in the case of $g_{\mathrm{CC}}(r)$ the theory predicts somewhat less structure than seen in the simulations. This is consistent with previous work [39] on an explicit atom model for polyethylene (PE) liquids and reflects the fact that PRISM theory is least accurate in predicting correlations between backbone sites that are shielded, in this case by the attached hydrogen atoms. It is instructive to directly compare the CC, HH, and CH intermolecular correlation functions in PEO liquids with polyethylene liquids shown in Fig. (3). As can be seen the packing in PEO and PE melts is very similar, although more structure is seen in the PE $g(r)$'s. This is likely due to the greater flexibility of the PEO chain backbone that permits a wider range of intermolecular contacts and fewer preferred intermolecular distances.

We have demonstrated that PRISM theory gives good

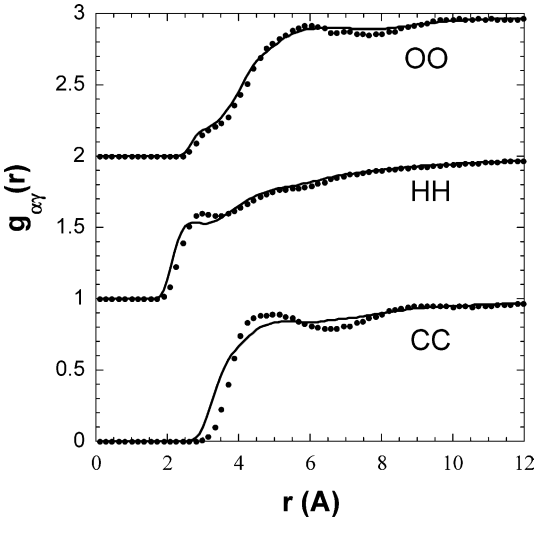

Fig. 1. Intermolecular radial distributions functions (between atoms of the same type) for PEO ($N=15$) in the liquid state at 318 K and density 0.1010 atoms/Å^3. Partial charges were turned off. Points—MD simulation, solid curves—PRISM theory. The curves are shifted along the y-axis for clarity.

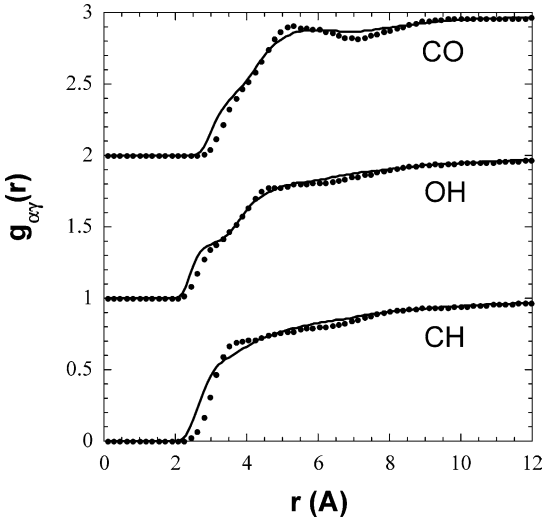

Fig. 2. Intermolecular radial distributions functions (between atoms of different types) for PEO ($N=15$) in the liquid state at 318 K and density 0.1010 atoms/Å^3. Partial charges were turned off. Points—MD simulation, solid curves—PRISM theory. The curves are shifted along the y-axis for clarity.

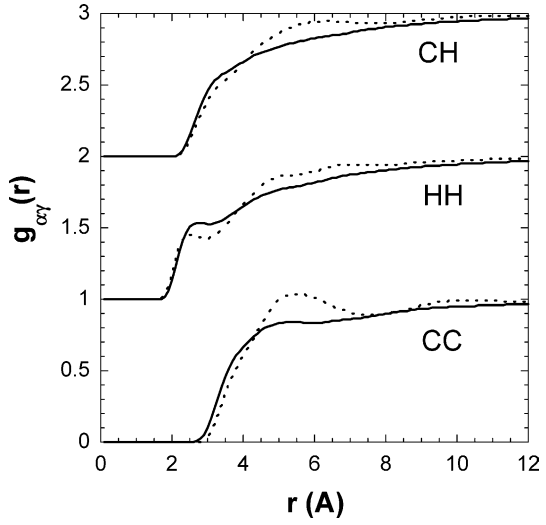

Fig. 3. Intermolecular pair correlation functions associated with C and H obtained from PRISM theory. Solid curves—PEO, $N=15$, $T=318$ K. Dotted curves—$C_{20}H_{40}$ from Ref. [39]. The curves are shifted along the y-axis for clarity.

agreement with MD simulations of PEO liquids when the Coulombic interactions are turned off. We now examine the effect of partial charges on the liquid packing. MD simulations were performed using the charges from the SJY potential given in Table 2. A comparison of the radial distribution functions with and without charges is given in Figs. (4) and (5). It can be seen that significantly more structure develops in pair correlations involving oxygen and carbon as a result of the charges. The partial charges also have a dramatic effect on the root-mean-square radius of gyration R_g. In Table 4 good agreement is seen in the R_g from MD and PRISM when the charges are turned off. However, when the charges are turned on the PEO chains significantly expand and R_g increases by 38%. Because the chains are more extended, additional intermolecular overlap is allowed between PEO macromolecules leading to the additional structure in the intermolecular radial distribution functions seen in Figs. (4) and (5).

The dramatic increase in R_g due to the charges presumably arises from long-range, Coulombic repulsions between like charges along the PEO chain backbone. From Table 2 it can be seen that the both C and O backbone atoms are negatively charged whereas the pendant hydrogens are positively charged to preserve neutrality. We can compute the intermolecular charge density about each of these atoms from the relation

$$\rho_{e\alpha}(r) = \sum_{\gamma} q_{\gamma} g_{\alpha\gamma}(r) \tag{12}$$

Results are shown in Fig. (6) based on the MD simulations. As can be seen the charge density is oscillatory with each atom on a given chain surrounded by positive charge in the 2.5–3.2 A regime due to the H atoms from other chains. The charge density changes to negative in the 5 Å region due to intermolecular C and O atoms. Finally, the charge density decays to zero on a 10–15 A length scale. In a recent study [24] on PDMS liquids, we found that the partial charges had a smaller effect on R_g and the intermolecular pair correlation functions, even though the magnitude of the charges is similar in the two macromolecules. However, in PEO each backbone C or O site is negatively charged, whereas in PDMS the Si and O atoms along the backbone are positive and negative, respectively. In PDMS this leads to less intermolecular Coulombic repulsion than we see in PEO.

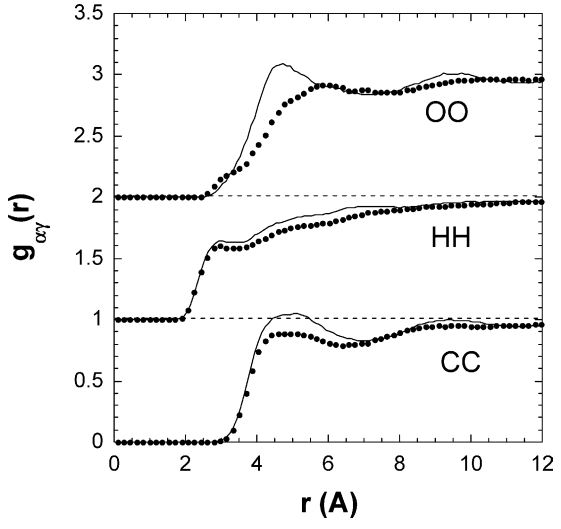

Fig. 4. PEO intermolecular radial distribution functions (between atoms of the same type) obtained from MD simulation. $N=15$, $T=318$ K, and density $=0.1010$ atoms/Å^3. Points—without charges, solid curves—with charges. The curves are shifted along the y-axis for clarity.

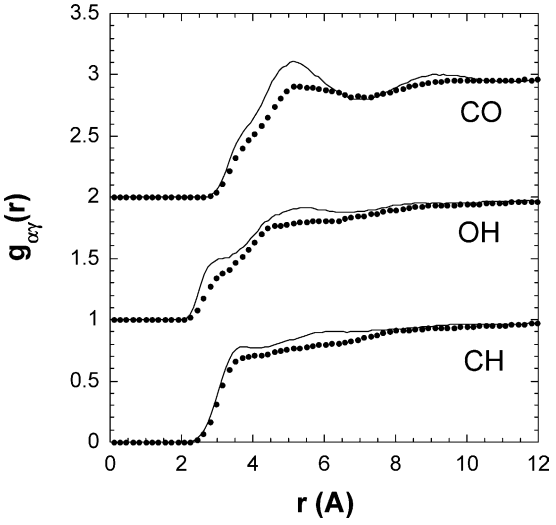

Fig. 5. PEO Intermolecular radial distribution functions (between atoms of different types) obtained from MD simulation. $N=15$, $T=318$ K, and density $=0.1010$ atoms/Å^3. Points—without charges, solid curves—with charges. The curves are shifted along the y-axis for clarity.

Wide angle neutron scattering has been used to study the structure of fully deuterated PEO liquids by two groups [20,21]. In Fig. (7) we show the structure factor $H(k)$ of PEO at 363 K reported by Annis et al. [20] defined according to

$$H(k) = \frac{I(k) - S_{self}}{\left(\sum_{\alpha} x_{\alpha} b_{\alpha}\right)^2} \tag{13}$$

where x_α and b_α are the atomic fraction and coherent neutron scattering length of atoms of type α in a monomer. In Eq. (13) the self-scattering $S_{self} = \sum_\alpha x_\alpha b_\alpha^2$ is subtracted from the total differential neutron scattering cross section per atom $I(k)$. The factor in the denominator normalizes the scattering to a monomer basis. The coherent scattering lengths for C and O in natural abundance and for H^2 were taken from Ref. [40].

We performed self-consistent PRISM calculations for PEO liquids of 54 monomers at $T=363$ K at the

Table 4
Radius of gyration of PEO chains

	MD (full)	MD (no charge)	PRISM
R_g (Å)	9.91±0.07	7.37+0.10	7.6

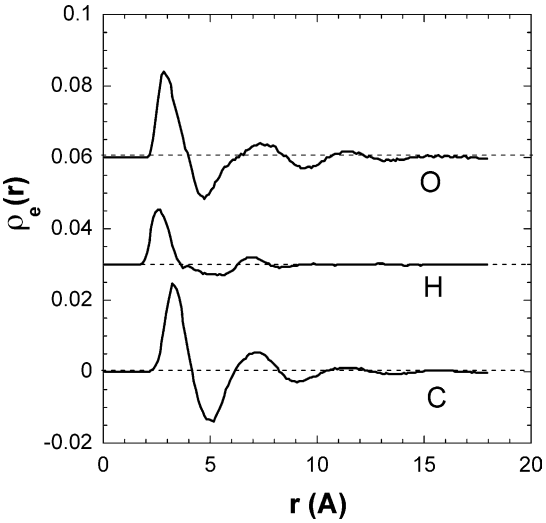

Fig. 6. The intermolecular charge distribution around each atom in PEO calculated from Eq. (12). The curves are shifted along the y-axis for clarity.

experimental density of 0.103 atoms/Å^3. As before, the charges were turned off in the PRISM calculation. The scattering intensity $I(k)$ was calculated from

$$I(k) = \sum_{\alpha\gamma} x_\alpha b_\alpha b_\gamma \hat{\mathbf{S}}_{\alpha\gamma}(k)/\rho_\alpha \tag{14}$$

using the partial structure factors defined in Eq. (8). Eq. (13) was then employed to obtain an estimate of $H(k)$. A comparison of PRISM theory with the neutron scattering experiments is shown in Fig. (7). The differences between theory and experiment are due to inaccuracies of the theory and the SJY potentials, but are primarily due to the effect of omitting the partial charges in the PRISM calculation. Also shown in Fig. (7) are MD simulations reported in Ref. [20] using the full SJY force field. Note that as in the case of the $g(r)$'s in Figs. (4) and (5), the inclusion of charges in the MD simulation leads to additional structure in $H(k)$ relative to the theory. Refinements were made to the SJY force field by Borodin et al. in a later study [12] which, when used in an MD simulation [12] of PEO liquids, is in quantitative agreement with the neutron scattering measurements [20] of Annis et al.

A useful feature of wide angle neutron scattering [20,41] is that the pair correlation function $g_{\mathrm{HH}}(r)$ between the hydrogen atoms can be directly extracted from experiments on hydrogenated and deuterated samples. Previously, both PRISM theory [39] and MD simulations were compared with experimental [41,42] $g_{\mathrm{HH}}(r)$ for polyethylene and alkane liquids. Here we make a similar comparison with the data of Annis [20] for PEO liquids. This comparison is shown in Fig. (8) as the Fourier transform of the total correlation function

$$h_{\mathrm{HH}}(r) = g_{\mathrm{HH}}(r) - 1 \tag{15}$$

As in the case of the total structure factor $H(k)$, we likewise see that PRISM theory predicts less structure than experiment for the HH correlations. Also shown in Fig. (8) is the MD simulation reported in Ref. [20] with the full SJY force field. In view of our earlier results it is not surprising that PRISM theory, with no charges, also predicts less structure in $\mathbf{h}_{\mathrm{HH}}(r)$ than the MD simulation with charges.

4. Conclusions

Our main finding in this study is that the partial charges surrounding the atoms have a significant effect on the chain

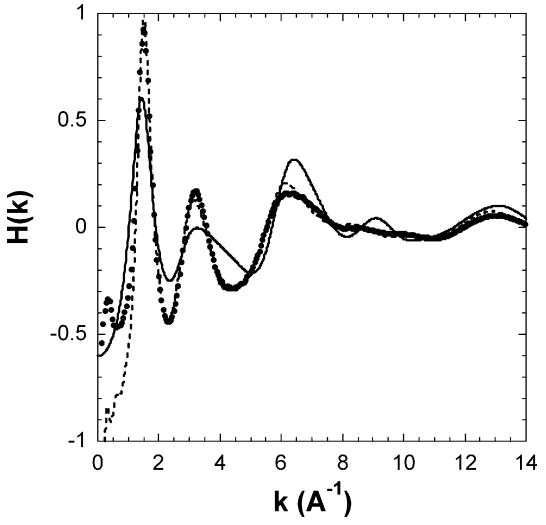

Fig. 7. The total structure function $H(k)$ defined in Eq. (13) for PEO liquid at 363 K. Points are from the wide angle neutron diffraction experiments of Annis et al. [20]. Solid curve—PRISM theory ($N=54$, $T=363$ K) with charges off. Dashed curve—MD simulations from Ref. [20] ($N=54$, $T=363$ K) with charges on.

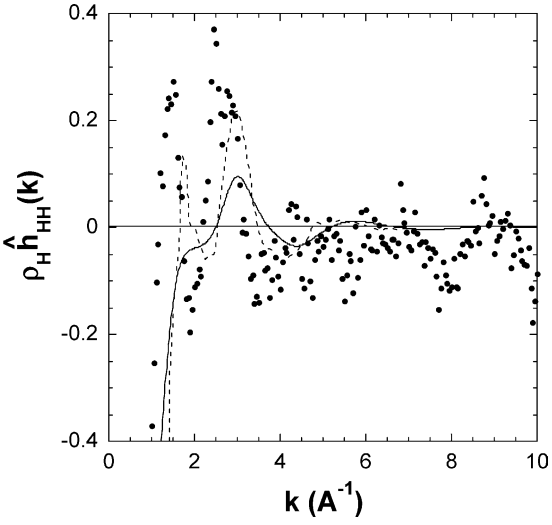

Fig. 8. The HH pair correlation function defined in Eq. (15) (in Fourier space) for PEO liquid at 363 K. Points are from the wide angle neutron diffraction experiments of Annis et al. [20]. Solid curve—PRISM theory ($N=54$, $T=363$ K) with charges off. Dashed curve—MD simulations from Ref. [20] ($N=54$, $T=363$ K) with charges on.

dimensions and intermolecular packing in poly(ethylene oxide) liquids. This effect is not seen in poly(dimethyl siloxane) liquids even though the magnitude of the charges in the two systems are comparable. The different responses may be related to the fact that in PEO all atoms on the chain backbone are negatively charged and the intramolecular Coulombic repulsions may be long range. In the case of PDMS, the backbone atoms alternate in the sign of the charge, which may cause the Coulombic repulsions to be screened to a larger degree than in PEO. Since the individual PEO chains become extended as a result of the charges, there is more intermolecular overlapping of chains in the liquid, which is reflected in more structure in the corresponding intermolecular radial distribution functions.

In PEO liquids without partial charges, there is very good agreement between self-consistent PRISM theory and MD simulations. PRISM theory, when used with the Percus-Yevick closure of Eq. (4), is most accurate for macromolecular liquids with strong repulsions and weak attractions. Hence, this PRISM/PY approach is probably not appropriate for describing macromolecular liquids with strong Coulombic interactions. Other molecular closures [22,43] have been used successfully in describing the effect of attractions on liquid structure. Another approach using PRISM theory, which is beyond the scope of this investigation, is to include the full Coulombic interactions in the single chain simulation part of the self-consistent calculation but retaining the repulsive PY closure.

Acknowledgements

Sandia is a multiprogram laboratory operated by Sandia Corporation, a Lockheed Martin Company, for the United States Depart of Energy's National Nuclear Security Administration under Contract DE-AC04-94AL85000. The authors would like to thank Brian Annis, Grant Smith, and Oleg Borodin for helpful discussions.

References

[1] Lumley JL. Ann Rev Fluid Mech 1969;1:367.
[2] Gray FM. Polymer electrolytes. Cambridge: Royal Society of Chemistry; 1997.
[3] Harris JM, editor. Poly(ethylene glycol) chemistry: biotechnical and biomedical applications. New York: Plenum Press; 1992.
[4] Karlstrom G. J Phys Chem 1985;89:4962.
[5] Linse P. Macromolecules 1993;26:4437.
[6] de Gennes PG. C R Acad Sci Paris II 1991;117:313.
[7] Matsuyama A, Tanaka F. Phys Rev Lett 1990;65:341.
[8] Bekiranov S, Bruinsma R, Pincus P. Phys Rev E 1997;55:577.
[9] Dormidontova EE. Macromolecules 2002;35:987.
[10] Semenov AN, Rubinstein M. Macromolecules 1998;31:1373.
[11] Smith GD, Bedrov D. J Phys Chem A 2001;105:1283. Smith GD, Bedrov D. J Phys Chem B 2003;107:3095.
[12] Borodin O, Douglas R, Smith GD, Trouw F, Petrucci S. J Phys Chem B 2003;107:6813.
[13] Smith GD, Borodin O, Bedrov D. J Comp Chem 2002;23:1480.
[14] Bin L, Boinske PT, Halley JW. J Chem Phys 1996;105:1668.
[15] Halley JW, Duan Y, Nielsen B, Redfern PC, Curtiss LA. J Chem Phys 2001;115:3957.
[16] Muller-Plathe F, van Gunsteren WF. J Chem Phys 1995;103:4745.
[17] Hyun JK, Dong H, Rhodes CP, Frech R, Wheeler RA. J Phys Chem B 2001;105:3329.
[18] Smith GD, Jaffe RL, Yoon DY. J Phys Chem 1993;97:12752.
[19] Annis BK, Kim M, Wignall GD, Borodin O, Smith GD. Macromolecules 2000;33:7544.
[20] Annis BK, Borodin O, Smith GD, Benmore CJ, Soper AK, Londono JD. J Chem Phys 2001;115:10998.
[21] Johnson JA, Saboungi DL, Price DL, Ansell S, Russell TP, Halley JW, et al. J Chem Phys 1998;109:7005.
[22] Schweizer KS, Curro JG. Adv Chem Phys 1997;98:1.
[23] Sides SW, Curro JG, Grest GS, Stevens MJ, Soddemann T, Habenschuss A, et al. Macromolecules 2002;35:6455.
[24] Frischknecht AL, Curro JG. Macromolecules 2003;36:2122.
[25] Schweizer KS, Curro JG. Phys Rev Lett 1987;58:246.
[26] Curro JG, Schweizer KS. Macromolecules 1987;20:1928.
[27] Curro JG, Schweizer KS. J Chem Phys 1987;87:1842.
[28] Heine DR, Grest GS, Curro JG. Adv Polym Sci 2004;176:211.
[29] Chandler D, Andersen HC. J Chem Phys 1972;57:1930.
[30] Chandler D. In: Montroll EW, Lebowitz JL, editors. Studies in statistical mechanics, vol. VII. Amsterdam: North-Holland; 1982.
[31] Hansen JP, McDonald IR. Theory of simple liquids. London: Academic Press; 1986.
[32] Weeks JD, Chandler D, Andersen HC. J Chem Phys 1971;54:5237.
[33] Pütz M, Curro JG, Grest GS. J Chem Phys 2001;114:2847.
[34] Chandler D, Singh Y, Richardson DM. J Chem Phys 1984;81:1975.
[35] Nichols AL, Chandler D, Singh Y, Richardson DM. J Chem Phys 1984;81:5109.
[36] Flory PJ. J Chem Phys 1949;17:203.
[37] Plimpton SJ. J Comput Phys 1995;117:1.
[38] Hockney R, Eastwood J. Computer simulations using particles. New York: Adam Hilger; 1988.
[39] Tsige M, Curro JG, Grest GS, McCoy JD. Macromolecules 2003;36:2158.
[40] Neutron News 1992;3:29. http://www.ncnr.nist.gov/resources/n-lengths/list.html.
[41] Londono JD, Annis BK, Turner JZ, Soper AK. J Chem Phys 1994;101:7868.
[42] Londono JD, Annis BK, Habenschuss A, Smith GD, Borodin O, Tso C, et al. J Chem Phys 1999;110:8786.
[43] Schweizer KS, Yethiraj A. J Chem Phys 1993;98:9053.